SANDIA REPORT

SAND2012-0124
Unlimited Release
Printed January 2012

Micro-Gas-Analyzer MEMS Active Pressure Valves Testing and Design

David Bonner and Paul Galambos

Prepared by
Sandia National Laboratories
Albuquerque, New Mexico 87185 and Livermore, California 94550

Sandia National Laboratories is a multi-program laboratory managed and operated by Sandia Corporation, a wholly owned subsidiary of Lockheed Martin Corporation, for the U.S. Department of Energy's National Nuclear Security Administration under contract DE-AC04-94AL85000.

Issued by Sandia National Laboratories, operated for the United States Department of Energy by Sandia Corporation.

Available to DOE and DOE contractors from
U.S. Department of Energy
Office of Scientific and Technical Information
P.O. Box 62
Oak Ridge, TN 37831

Telephone: (865) 576-8401
Facsimile: (865) 576-5728
E-Mail: reports@adonis.osti.gov
Online ordering: http://www.osti.gov/bridge

Available to the public from
U.S. Department of Commerce
National Technical Information Service
5285 Port Royal Rd.
Springfield, VA 22161

Telephone: (800) 553-6847
Facsimile: (703) 605-6900
E-Mail: orders@ntis.fedworld.gov
Online order: http://www.ntis.gov/help/ordermethods.asp?loc=7-4-0#online

SAND2012-0124
Unlimited Release
August 2011

Micro-Gas-Analyzer MEMS Active Pressure Valves Testing and Design

David Bonner
1749
Sandia National Laboratories
P.O. Box 5800
Albuquerque, New Mexico 87185-MS1080

Abstract:

Micro-Gas-Analyzers have many applications in detecting chemical compounds present in the air. MEMS valves are used to perform sampling of gasses, as they enable control of fluid flow at the micro level. Current generation electrostatically actuated MEMS valves were tested to determine their ability to hold off a given gauge pressure with an applied voltage. Current valve designs were able to hold off 98 psi with only 82 V applied to the valves. The valves were determined to be 1.83 times more efficient than older valve designs, due to increasing the electrostatic area of the valve and trapping oxide between polysilicon layers. Newer valve designs were also proposed and modeled using ANSYS multiphysics, which should be able to hold off 100 psi with only 29 V needed. This performance would be 2.82 times more efficient than current designs, or 5.17 times more efficient than older valve designs. This will be accomplished by further increasing the valve radius and decreasing the gap between the valve boss and electrode.

ACKNOWLEDGMENTS

I would like to thank Paul Galambos, my mentor for this project, as he provided guidance and insight. I would also like to thank Keith Ortiz and Tara Love-Archuletta, for their administrative help in putting this project and report together. Additionally, I would like to thank Jeff Lantz, Austin Welborn, and Mike Baker for their help in modeling and redesigning the valves. Thank you, Gayle Schwartz, Doug Chinn, and Adrian Wagner for your efforts in the packaging process. I would like to thank Jamie McClain and Ted Parson, for their aid in the experimental testing of the valves. Mike Shaw and Greg Bogart also contributed in helping me better understand the SUMMIT V process. Finally, I would like to thank my personal Lord and Savior, Jesus Christ, for all the blessings He has bestowed upon me, including the opportunity to work at Sandia.

Contents

FIGURES

Introduction:

Micro-Gas-Analyzers (MGAs) have a wide variety of applications, and are useful for detecting environmental hazards and toxic gasses. Performing gas analysis on the micro level is useful for atmospheric sampling in the field, as soldiers can use the portable devices to obtain real time data to detect a particular toxic gas. Because the devices are small, they can also be easily hidden, enabling their use in areas where gas detection is necessary, but where one wants the device to remain concealed, such as in an airport [1].

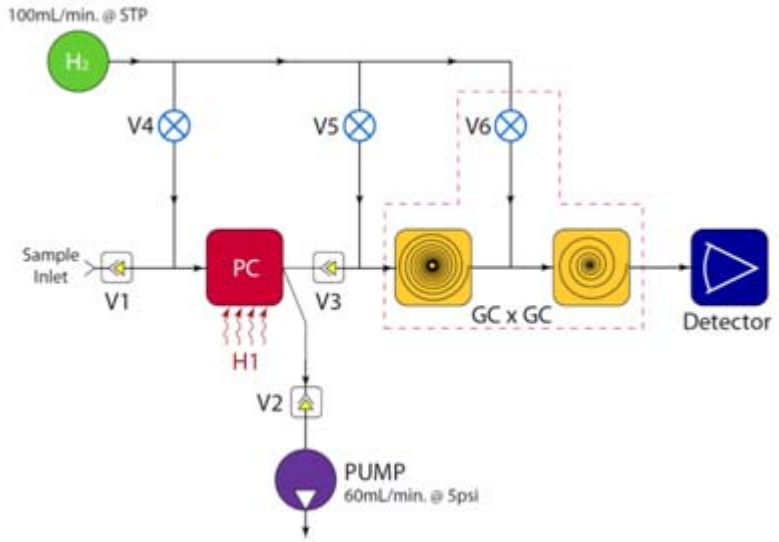

Figure 1, Schematic of an MGA assembly

A schematic of an MGA is shown in Figure 1. Typically, MGAs use gas chromatography (GC) to detect the presence of certain compounds, as they enable high sensitivity. The gas sampling is performed using both passive and active MEMS microvalves, as they enable rapid sampling and minimal interference with the GC analysis [2, 3]. The air flow into the gas chromatograph is accomplished by sampling the air using passive MEMS microvalves (shown as V1, V2, and V3). The air is passed through a pre-concentrator (PC), which allows the air to pass through, but traps chemical compounds. The pre-concentration step

is necessary to ensure a highly concentrated sample of the gas is passed into the GC, so its presence is detected. After sampling for a few seconds, the sample is then heated to release the compounds on the PC. Gas is then flowed to carry the compounds into the GC by using active pressure valves (shown as V4, V5, and V6). This paper focuses on the testing and design of the active MEMS pressure valves, as it is desirable to be able to seal a high amount of gas pressure using a low amount of applied voltage, as this enables low power consumption by the MGA system.

Valve Operation:

The active MEMS pressure valves (referred to as valves from now on) are electrostatically actuated, as a voltage differential is applied between the valve boss (a cylindrical diaphragm like device which moves upward and downward to ensure a seal is maintained) and the underlying substrate. The entire device is fabricated using standard SUMMIT V processing, with a few slight modifications. Figure 2 shows a typical valve as seen from above by a white light Wyco Interferometer. The valve boss (shown in red), is held above the surface of a substrate wafer plane (shown in blue) by 4 springs. Underneath the surface of the valve boss, there is a small diameter hole etched through the silicon, which enables air to flow through the device (air flow would be out of the page as shown). The two circles drawn in black are not present in the original image, but serve to illustrate valve features underneath the boss not visible from above. The seal ring is attached underneath the surface of the boss, and makes contact with the underlying substrate when the valve boss is actuated down (into the page). Because the diameter of the seal ring is greater than the diameter of the hole etched into the silicon to allow air flow, when the seal ring comes into contact with the substrate, air flow is prevented, creating a seal. The seal ring acts very much like an o-ring, as it does not allow air to escape around it. Additionally, an outer ring is present, which also makes contact with the substrate (however, the seal is achieved by the inner ring). The electrostatic region in which the voltage differential exists is located between the two rings, as shown. Because the two rings make contact with the substrate before the valve boss body, a gap is maintained between the valve boss and the electrode, enabling the voltage differential to exist.

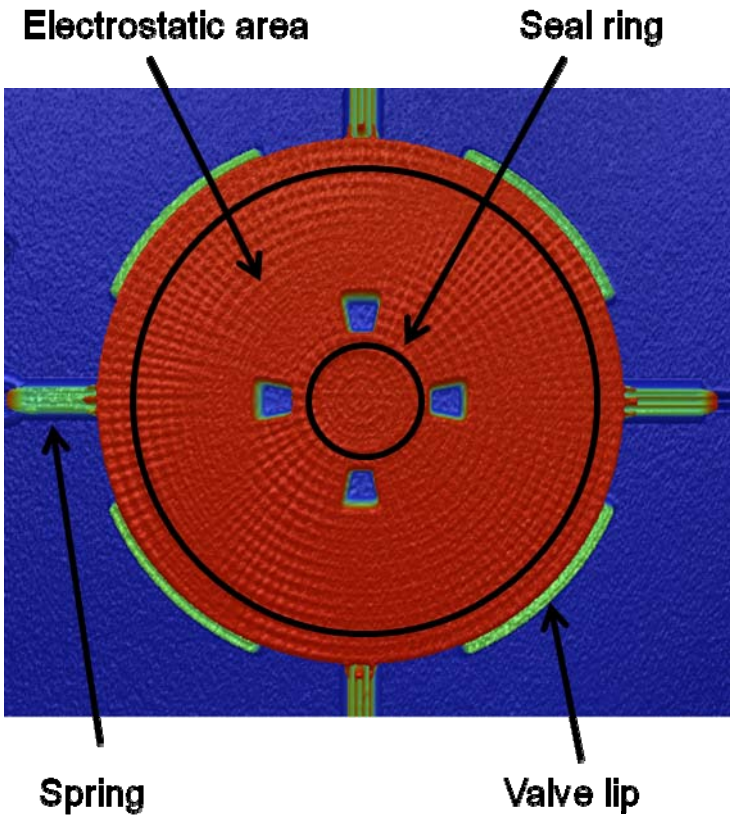

Figure 2, Wyco Interferometer image of a valve

Additional features of the valve include 4 holes in the valve boss (shown in blue), which allow air flow to be increased when the valve is open. Finally, the valve lips restrict the upward motion of boss, preventing the springs from over-displacing. Figure 3 shows an AutoCAD drawing of the device, (complete with bond pads which allow voltage connection), appearing as squares at the top and bottom of the device.

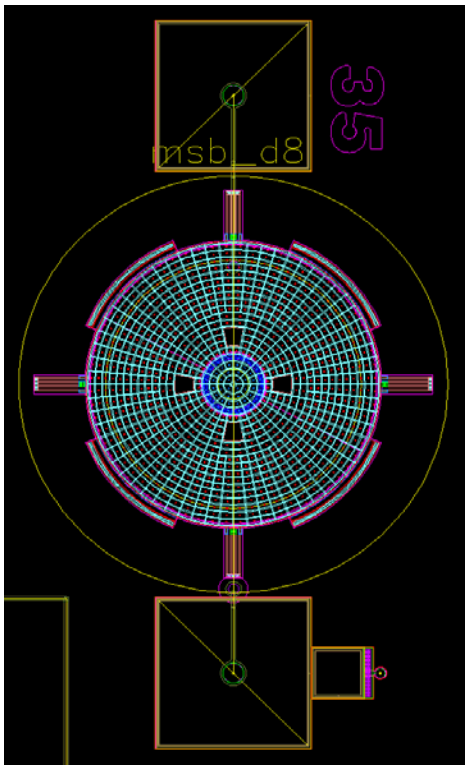

Figure 3, AutoCAD drawing of a valve

SUMMIT V Fabrication:

The valve is fabricated using all 5 layers of polysilicon, as shown in Figure 4, which gives a general overview of the SUMMIT process layers. The MMPOLY0 (all MMPOLY layers are made of polysilicon) layer is deposited and used as the electrode which experiences a voltage potential different from ground potential. The SACOX1 (sacrificial silicon dioxide, typically gets removed later) layer is deposited, and a dimple etch is performed. This effect results in the MMPOLY1 layer being non-planar, containing two protrusion rings, which serve as the seal ring and outer ring of the boss. The valve boss consists of the MMPOLY1, MMPOLY2, MMPOLY3, and a double thickness MMPOLY4 layer, with the oxide generally being removed from between the polysilicon layers. These polysilicon layers are electrically grounded to create the voltage differential between them and the MMPOLY0 layer. Some exceptions to this general

design occur, as in some cases it can be advantageous to trap sacrificial oxide between polysilicon layers, as will be explained later.

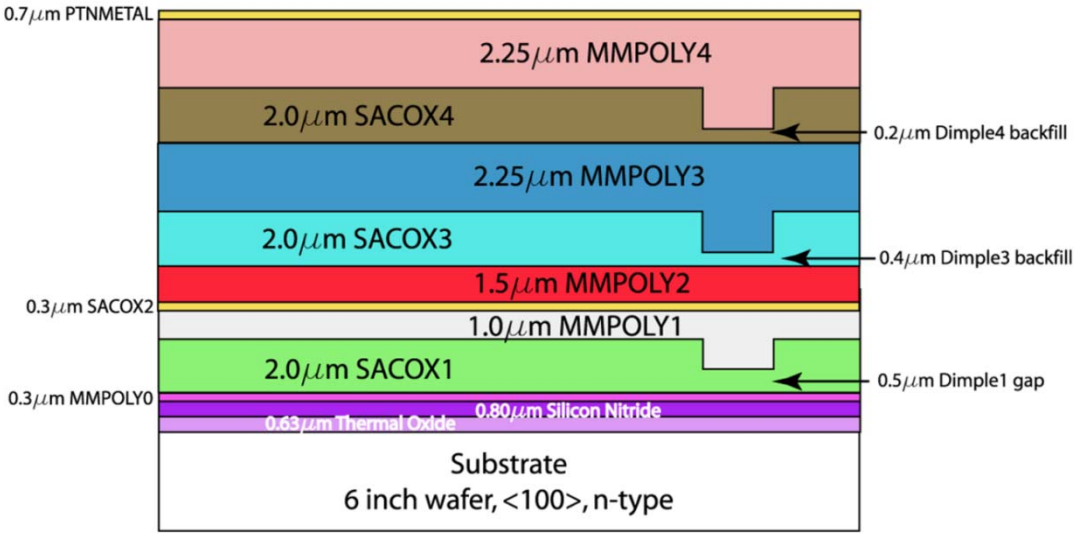

Figure 4, SUMMIT V process steps

Theoretical Background:

A free body diagram on a cross section of the boss is shown in Figure 5. The forces acting on the valve pertain to when the valve is sealed. The electrostatic force is the only force which pulls the boss down to seal the pressure against the substrate. When the boss is sealed, the inner seal ring and the outer ring are in contact with the substrate, and exert an upward force on the boss. The spring force is exerted upward, as the boss is displaced from equilibrium when sealed. The pressure force, resulting from the air pressure differential, acts upward only over the area inside the seal ring. The valve boss will remain sealed as long as the electrostatic force is greater than all of the upward forces.

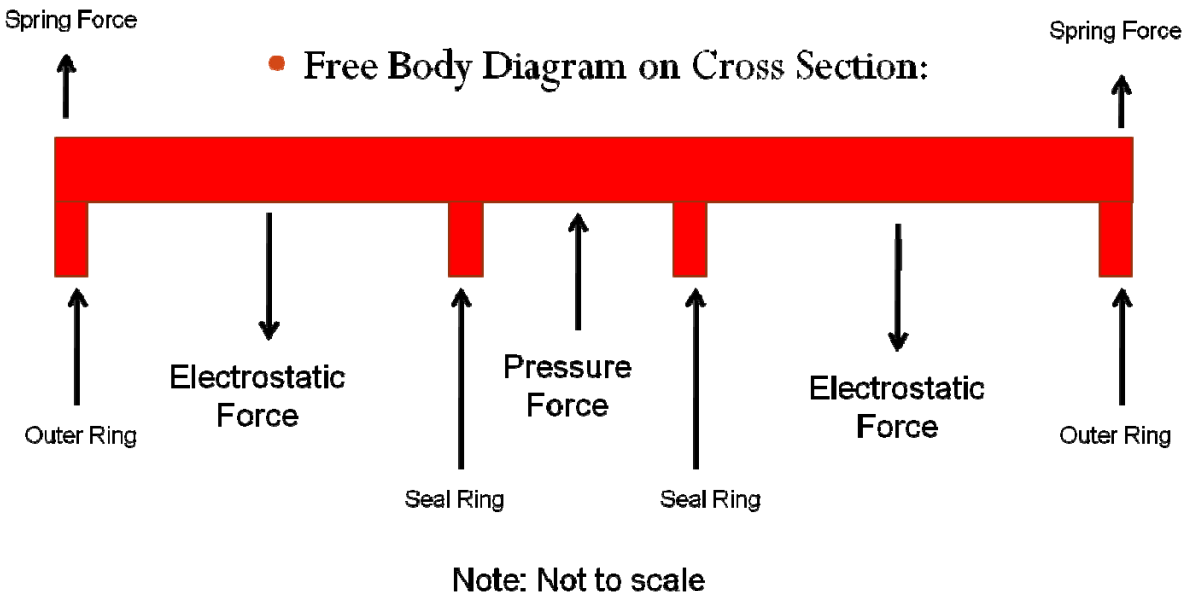

Figure 5, Free body diagram on cross section of valve when sealed

Figure 6 shows an ANSYS multiphysics (Finite Element Modeling Program) valve boss under both electrostatic and pressure loads. The red region represents the electrostatic region of the boss which is deforming downwards due to the electrostatic force. The blue region represents the upward deformation of the boss due to the applied pressure force inside the seal ring.

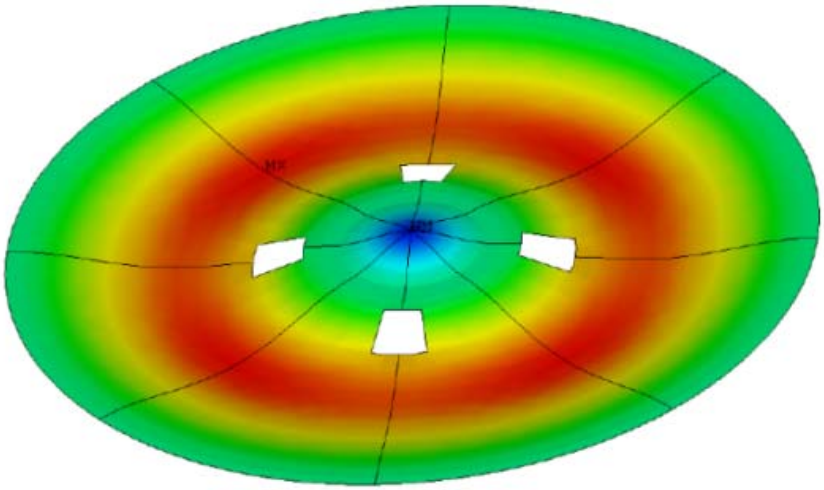

Figure 6, ANSYS model of valve

Figure 7 provides equations governing the forces acting on the valve boss. In the electrostatic force equation, ϵ is the dielectric constant, A is the area of the electrostatic region, V is the applied voltage, and d is the distance between the electrode and the valve boss. The area of the electrostatic region is determined by the valve radius. The variable d is determined by the dimple height of the SACOX1 etch, equivalent to the thickness of the seal and outer rings. In the force pressure equation, R_{seal} is the radius of the inner seal ring, and Pressure is the pressure exerted by the gas on the boss.

$$F_{electrostatic} = \frac{1}{2}\frac{\epsilon A V^2}{(d)^2}$$

$$F_{pressure} = \pi {R_{seal}}^2 * Pressure$$

Figure 7, equations governing forces on valve

Methods:

ANSYS Multiphysics Modeling

Because analytical modeling has limitations, ANSYS multiphysics, Finite Element Modeling Software, was used to model the valve performance. ANSYS is able to account for the coupled deflection/electrostatic force resulting from boss deformation. As the electrostatic force is applied, the valve boss deforms, which decreases the gap between the boss and the electrode, increasing the electrostatic force. Another advantage of ANSYS is that it enables one to rapidly test a variety of valve designs and predict their efficiencies.

A one eighth symmetry model was used to model the valve geometry, as this enables faster performance. Figure 8 shows the ANSYS valve symmetry model, with the red region representing electrostatic elements, the purple representing the seal elements, and the teal region showing the pressure elements.

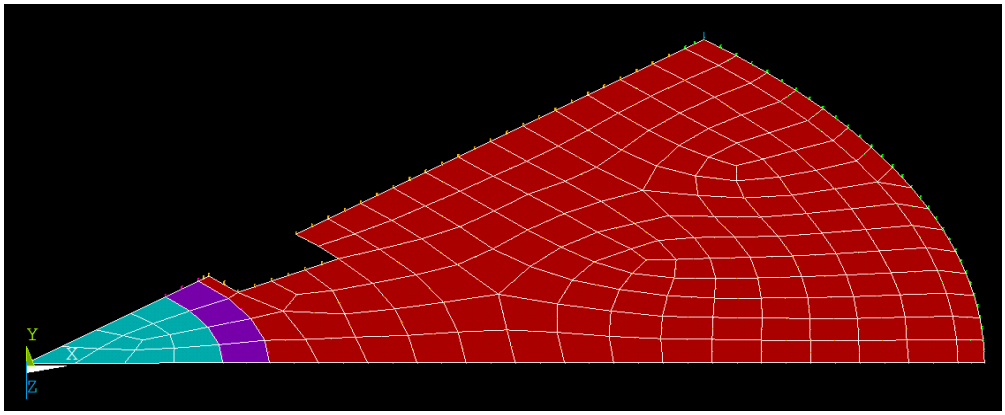

Figure 8, ANSYS one eighth symmetry model

ANSYS predicts when the valve fails by analyzing the force on the seal ring. When the force on the seal ring is zero, this indicates the seal is no longer in contact with the substrate. This in turn signifies the valve has lifted off due to the pressure force overcoming the electrostatic force.

Packaging

After the dies were released from the wafer, the valves were packaged for testing. The packaging requirements contained two criteria: each valve must have an isolated air pressure connection, and each valve must have a voltage connection. A ceramic plate with five drilled holes was fabricated as shown in Figure 9. This package enabled testing of all the valves with two configurations, as the valve pattern can be seen in Figure 10. The valves of interest include the 5 valves in the left column, and the middle 3 valves in the right column. One alignment would enable testing of 5 valves, and the other alignment the remaining 3. The drill holes were aligned with the centers of the valves, and epoxy was used to seal the valve die to the ceramic package. To isolate individual valves, a piece of tape was placed over the back face of the ceramic package, and a hole was punctured in the tape for the valve that was tested. The ceramic package was connected to a pressure system, so that the flow of air would be out of the page as shown. After sealing the dies to the ceramic package, wire bonds were then used to make a voltage connection to each valve for the application of electrostatic force.

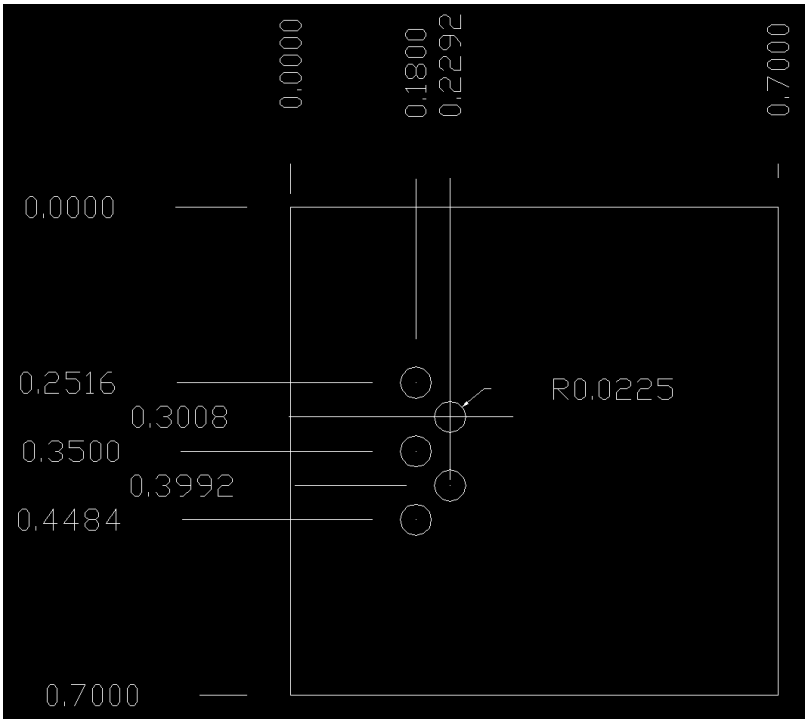

Figure 9, AutoCAD drawing of ceramic package

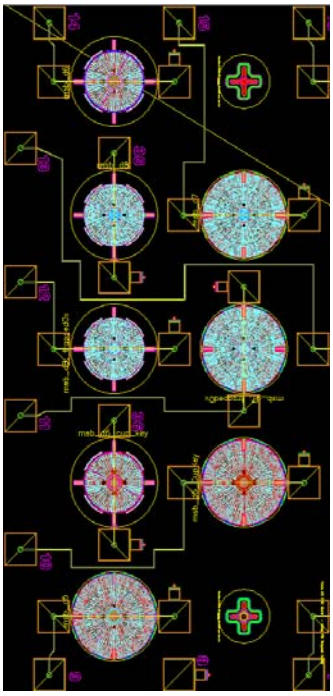

Figure 10, AutoCAD drawing of valve layout

Experimental setup:

A schematic of the testing setup is shown in Figure 11. The blue boxes represent pressure connections to the valve, and the green boxes represent voltage connections to the valve. The first step in the testing procedure was to apply a voltage to the device, such that the valve sealed. This was detected by using a Wyco Interferometer, as the distance between the top of the valve boss and the underlying substrate was seen to change with an applied voltage, indicating the valve boss had moved downward and the seal ring was in contact with the substrate. Air pressure was then increased to a specified value, using a pressure regulator and a digital pressure gauge. A flowmeter was used to detect the amount of air flowing through the system. When the valve was sealed, a very low amount of flow was observed, less than 1 mL/min. After the valve was sealed and the pressure was applied, the voltage was slowly decreased until the valve lifted off of the substrate, indicating the seal had failed. Upon failure, the flow was seen to increase to a much higher value, indicating the seal was no longer maintained. This procedure was repeated for varying voltage and pressure values.

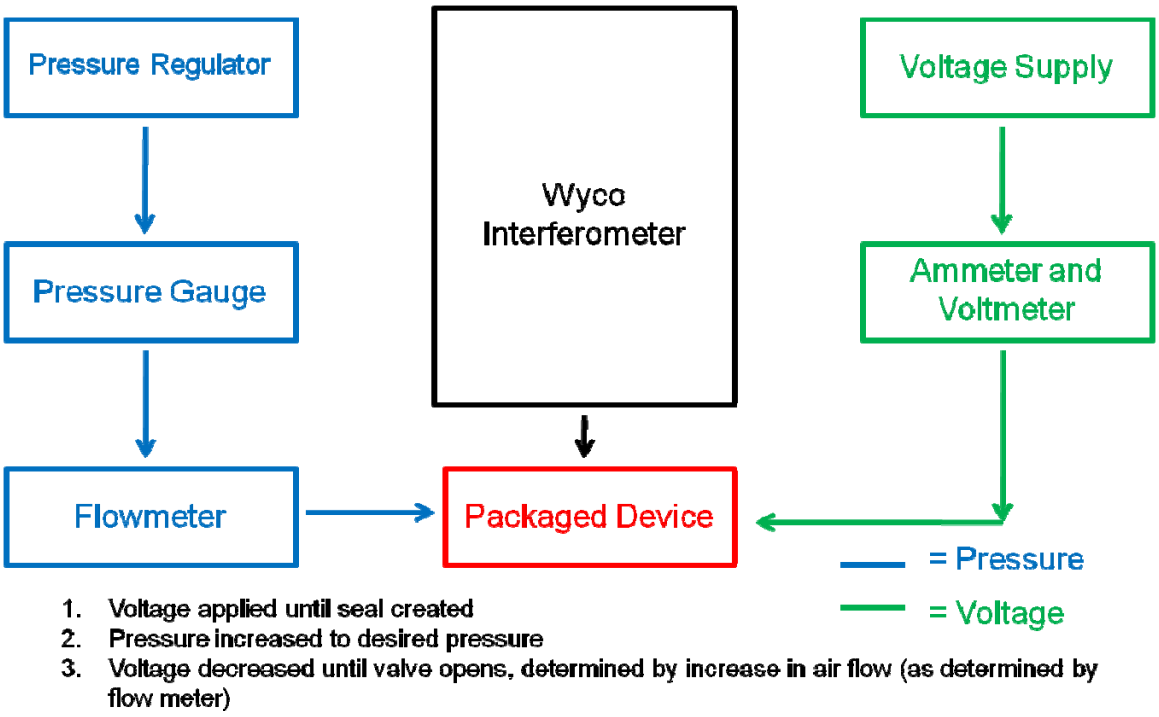

Figure 11, schematic of testing setup

Results and Discussion:

Valve Testing:

Figure 12 shows the experimental data taken for a variety of valves. The graph shows the point at which the valve was no longer able to seal against a certain pressure with an applied voltage. The small radius valves had a radius of 288 microns. The large radius valves had a radius of 400 microns. All valves had a dimple height of 1 micron, fixing the gap between the boss and the electrode at 1 micron when the valve was sealed. Other valve modifications existed, including different sealing mechanisms and thicknesses at the valve centers. Valve 7 is the most efficient design. Its ability to hold off close to 100 psi with only 82 V is a significant improvement over previous valve designs, which required around 150 V to accomplish this feat. Thus, valve 7 is $\frac{150\text{V}}{82\text{ V}} = 1.83$ times more efficient than the previous generation of valves.

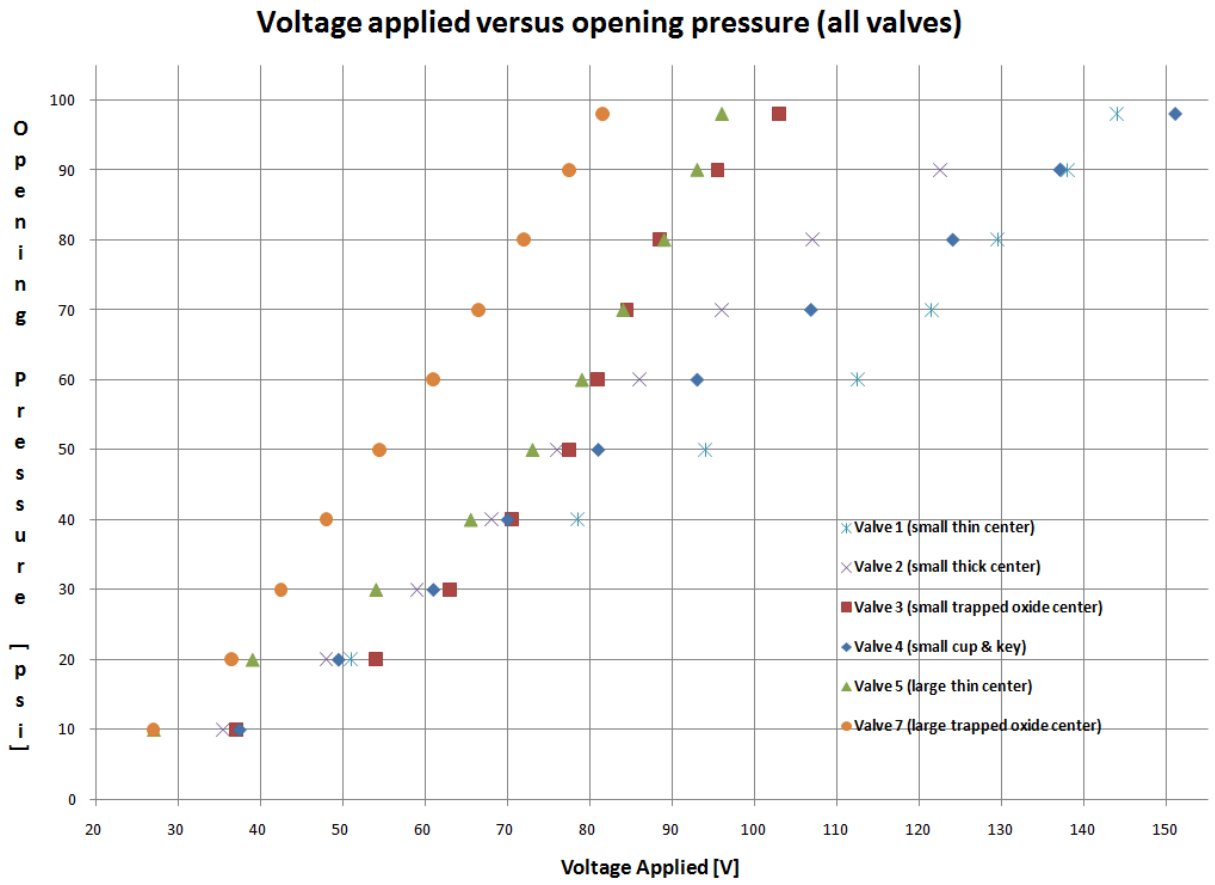

Figure 12, Experimental data for all valves

Two main trends are apparent. The larger radius valves performed better than the smaller radius valves. Also, the valves with trapped oxide in their centers performed better than valves without trapped oxide present.

Both of the large radius valves (valves 5 and 7) were able to hold off close to 100 psi with less than 100 V being applied, whereas the smaller radius valves (valves 1-4) required more than 100 V to hold off 100 psi. This effect can be explained due to the larger electrostatic area the larger valves have, which generates a larger electrostatic force per a given voltage, as shown in the first equation of Figure 7.

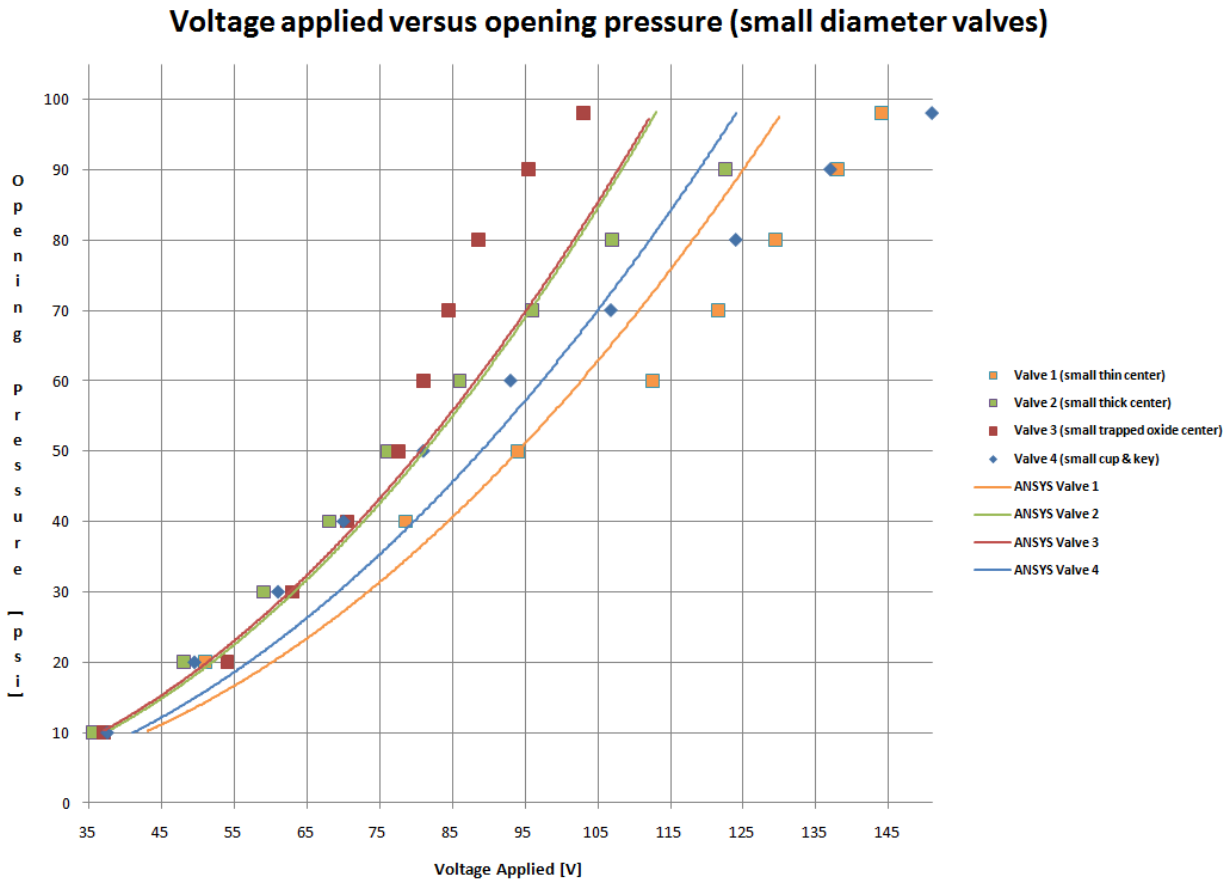

Figure 13, Experimental data and ANSYS simulations for small valves

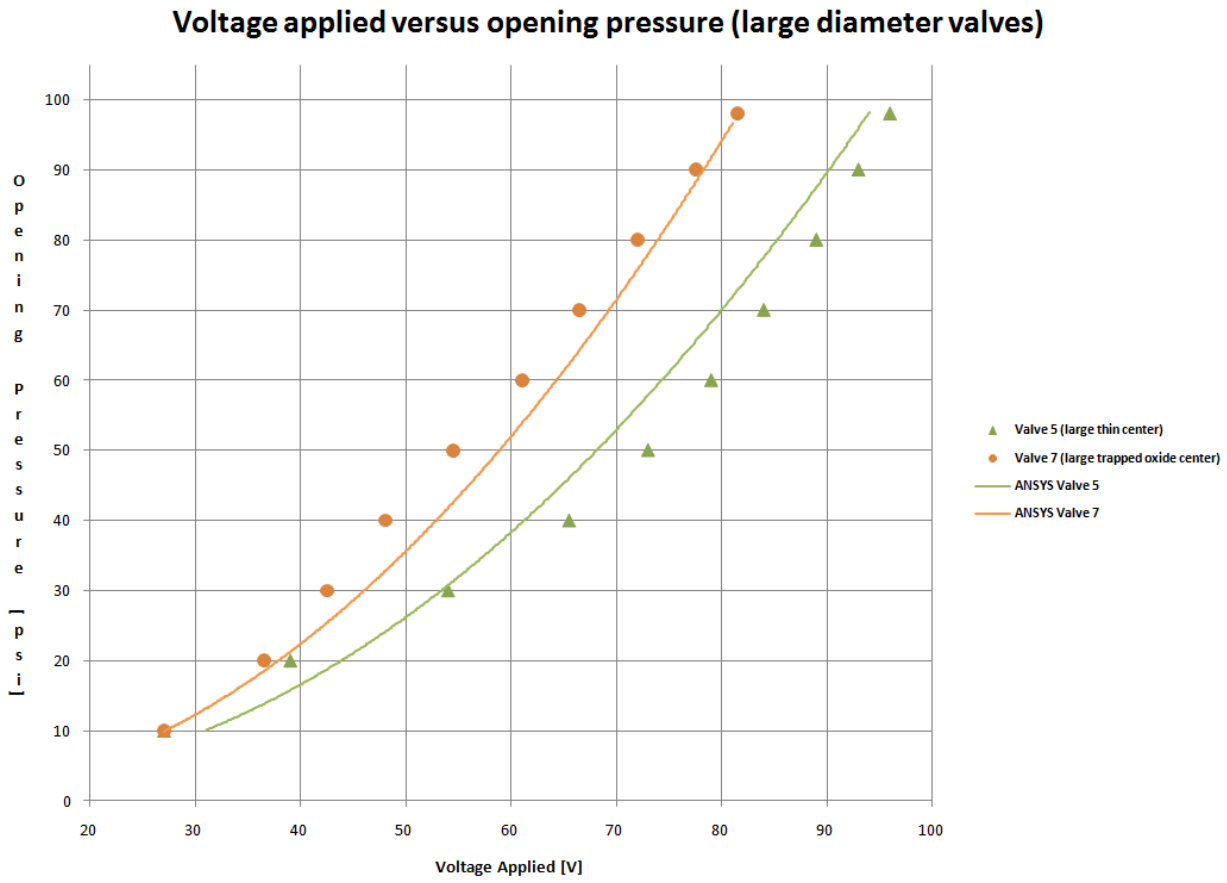

Figure 14 Experimental data and ANSYS simulations for large valves

Figures 13 and 14 show data re-plotted for the small radius valves and the large radius valves, respectively. The data points are the experimental results from Figure 12, and the curves are the ANSYS simulations for each valve. The ANSYS models predicted the valve performance effectively, as their curves closely match the data.

Notice that the valves with trapped oxide present (valve 3 in Figure 13, and valve 7 in Figure 14) performed better than valves without trapped oxide (valves 1, 2, and 4 in Figure 13, and valve 5 in Figure 14). The trapped oxide valves also performed better than the ANSYS model predicted, as they are to the left of the ANSYS curve. However, the valves without trapped oxide present did not perform as well as the ANSYS model predicted, as they required a

higher than predicted voltage to hold off a given pressure. This effect can be explained by Figure 15.

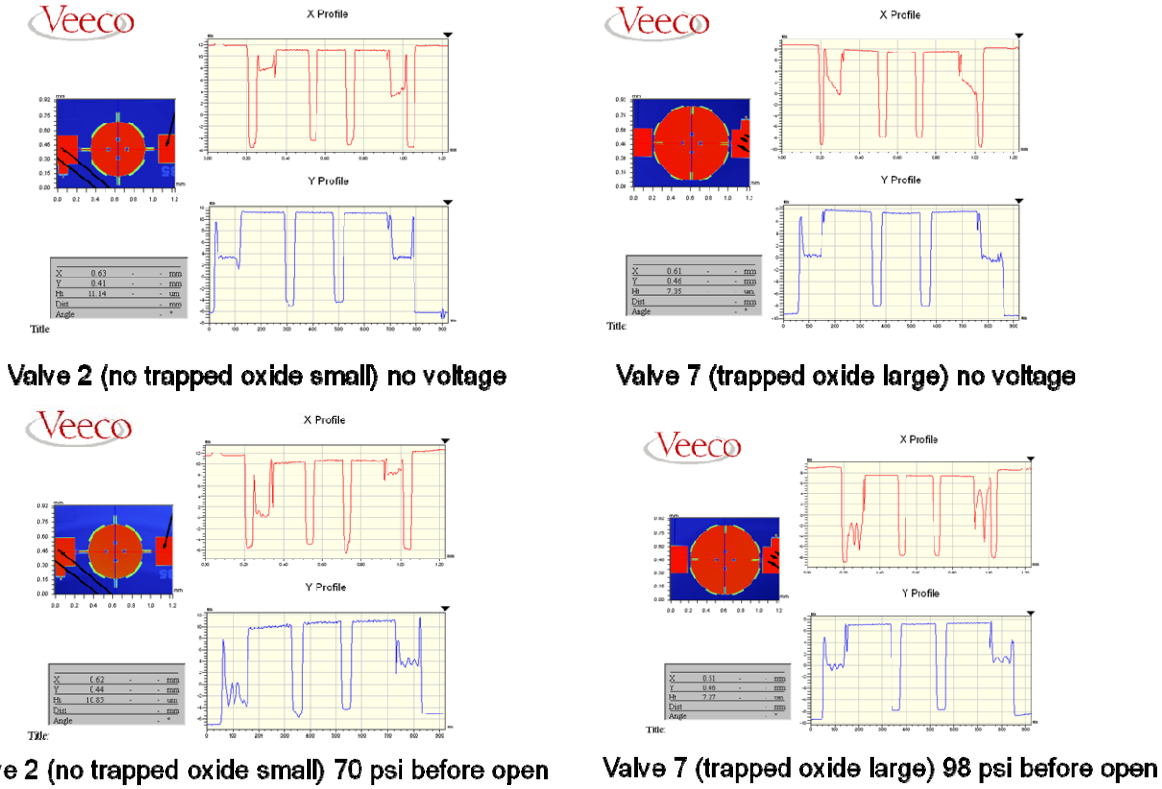

Figure 15, Wyco images for valves with and without trapped oxide, under varying loading conditions

The left column shows two cross sectional views of a valve that does not contain trapped oxide in its center (image generated from a Wyco Interferometer). The right column shows views of a valve that does contain trapped oxide in the valve center. The top row shows the respective valves with no applied voltage and no applied pressure. The bottom row shows the valves under both voltage and pressure loading when the valve is sealed. Notice how the valve without the trapped oxide is horizontal when no load is applied, but bows upward at its center when both voltage and pressure are applied. The valve with the trapped oxide bows downward when no loading is applied, and is horizontal when voltage and pressure are applied. This could

be a contributing factor, explaining why the valve with trapped oxide performs better than the valve without trapped oxide.

For after valve sealing, the pressure force at high pressures has a significant effect on valve deformation, and thus bows the valve upward from its original orientation. When the valve is no longer horizontal but is bowing upward at high pressures, the seal ring underneath the valve is no longer perpendicular to the substrate. Thus, it is possible that the seal is not performing to its full potential in the valve without the trapped oxide, contributing to the valve opening prematurely. The valve with the trapped oxide does not experience this problem, as its center is horizontal and its seal remains perpendicular to the substrate at high pressures.

Problems encountered in testing

One of the most significant problems encountered in testing microvalves was the presence of stringers. A stringer is a piece of silicon nitride or polysilicon that gets removed along with the sacrificial oxide in a release step performed during SUMMIT V processing. These stringers can become lodged in the devices, creating complications. A stringer can bridge the gap between the valve boss and the underlying electrode, causing a current short. This results in difficulty achieving a voltage potential between the boss and the electrode, preventing the valve from sealing. A stringer shown at 10 x magnification is seen in Figure 16, and a stringer at 50 x magnification is seen in Figure 17.

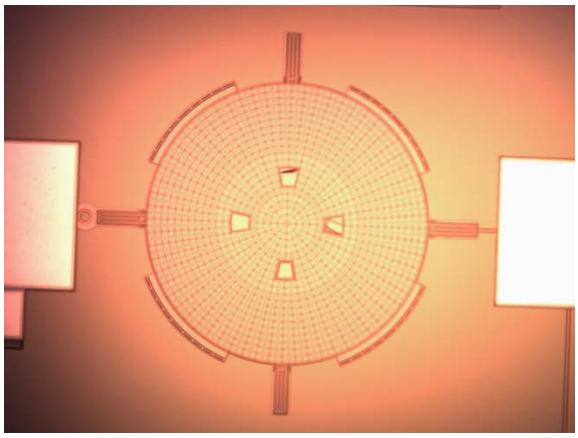

Figure 16, 10 times magnification for valve with stringers present

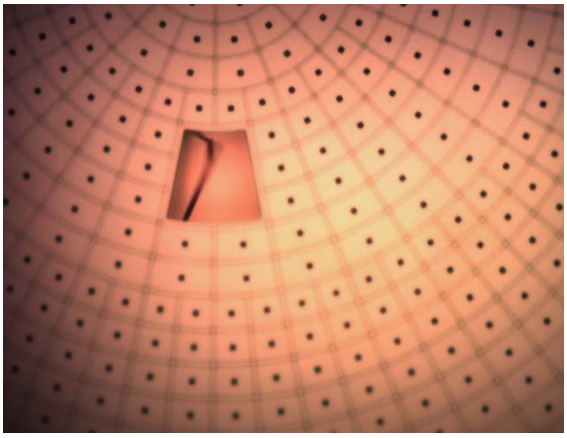

Figure 17, 50 times magnification for valve with stringer present

Another problem encountered in valve testing included valve springs getting stuck in their upward positions. When the valve is sealed and the pressure force overcomes the electrostatic force at failure, the valve lifts off. This process can be violent at pressures above 70 psi. The valve boss will travel upward until it contacts the valve lips, which allow for around 2 microns of valve travel. Oftentimes, one of the four springs will become stuck in the upward position, in such a way that the valve is unable to seal even when voltage is again applied. Figure 18 shows a Wyco generated image of a valve with one of its springs stuck. Notice on the red chart, the large degree of slanting across the valve boss when voltage is applied. The spring on the right side of the valve is preventing the boss from deflecting downward on that side,

whereas the other springs allow the boss to travel downward. Thus, the slanting effect is observed, and the valve boss is prevented from sealing in future tests.

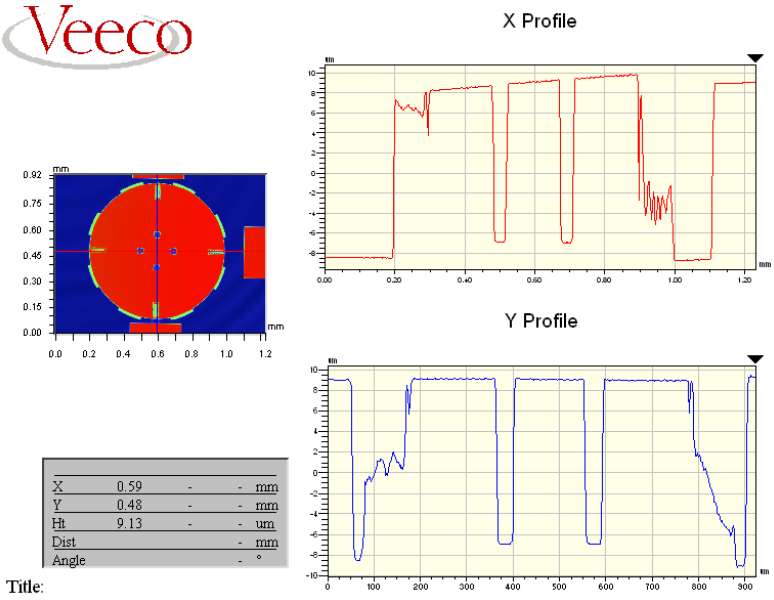

Figure 18, Wyco image for valve with spring stuck

Future Designs

The current generation valves were efficiently modeled using ANSYS; thus, it was deemed appropriate to design a new set of microvalves using ANSYS to determine the most efficient valve geometry. Figure 19 shows a graph with the predicted performance of 4 sets of valves that will be fabricated in the future. All of the valves will have a dimple height of .4 micrometers, less than the current generation of valves which have a dimple height of 1 micrometer. Shortening the dimple height is equivalent to reducing the gap between the valve boss and electrode when the valve is sealed, which provides a greater electrostatic force. Figure 19 shows the performance of 4 different sized radius valves, all of them modeled without trapped oxide present. Notice the largest radius valve (550 micrometers) is predicted to be unable to hold off 100 psi. All of the other valves are predicted to be able to hold off pressure greater than

100 psi, although their performance above this pressure range is not plotted. This can be explained by the tradeoff in increasing the electrostatic force (which effectively increases efficiency) and creating a robust design. When the dimple height is decreased and the radius is increased, the deformation of the valve boss towards the electrode is increased. If the deformation exceeds a certain value, pull in occurs, bringing the boss into contact with the electrode, causing a voltage short, which results in the valve opening. Thus, there is a tradeoff in increasing valve efficiency and creating a valve that is robust, as it is not desirable to be close to the pull in point to hold off a certain pressure. Concordantly, the 550 micrometer radius valve is the most efficient design but the least robust, and the 400 micrometer radius valve is the least efficient design but is the most robust. A number of valve geometries were analyzed, and these were determined to be the most efficient designs. The 500 micrometer radius valve is predicted to be $\frac{82V}{29V} = 2.82$ times more efficient than the current valve designs, as it should hold off 100 psi with only 29 applied Volts. It is also noteworthy that in the testing of the current generation valves, the valves with trapped oxide outperformed their ANSYS models. Thus, it is possible that the new generation valves with trapped oxide present in the valve centers could perform even better than these ANSYS curves predict.

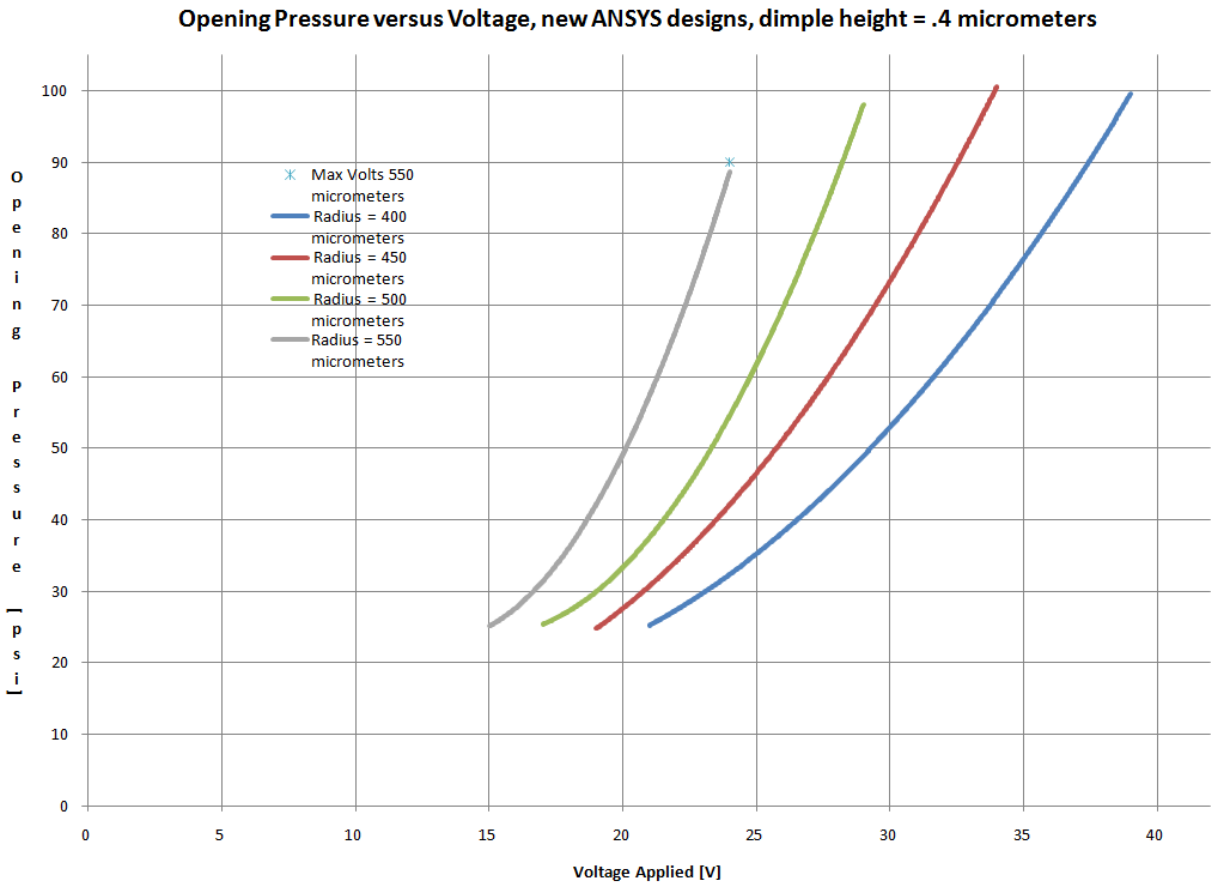

Figure 19, ANSYS simulation for newly designed valves

AutoCAD Designs

Using the valve designs analyzed using ANSYS, AutoCAD was used to design and draw these new generation valves, shown in Figure 20. Each row shows a particular valve radius, with the 400 micrometer valves shown on top, and the 550 micrometer valves shown on the bottom. The left column valves will be fabricated without trapped oxide in the center. The middle column and right column will be fabricated with 1 layer of trapped oxide (between poly1/2 laminate and poly 3), and 2 layers of trapped oxide (between poly1/2 laminate and poly 3, and between poly3 and poly4), in the valve centers, respectively.

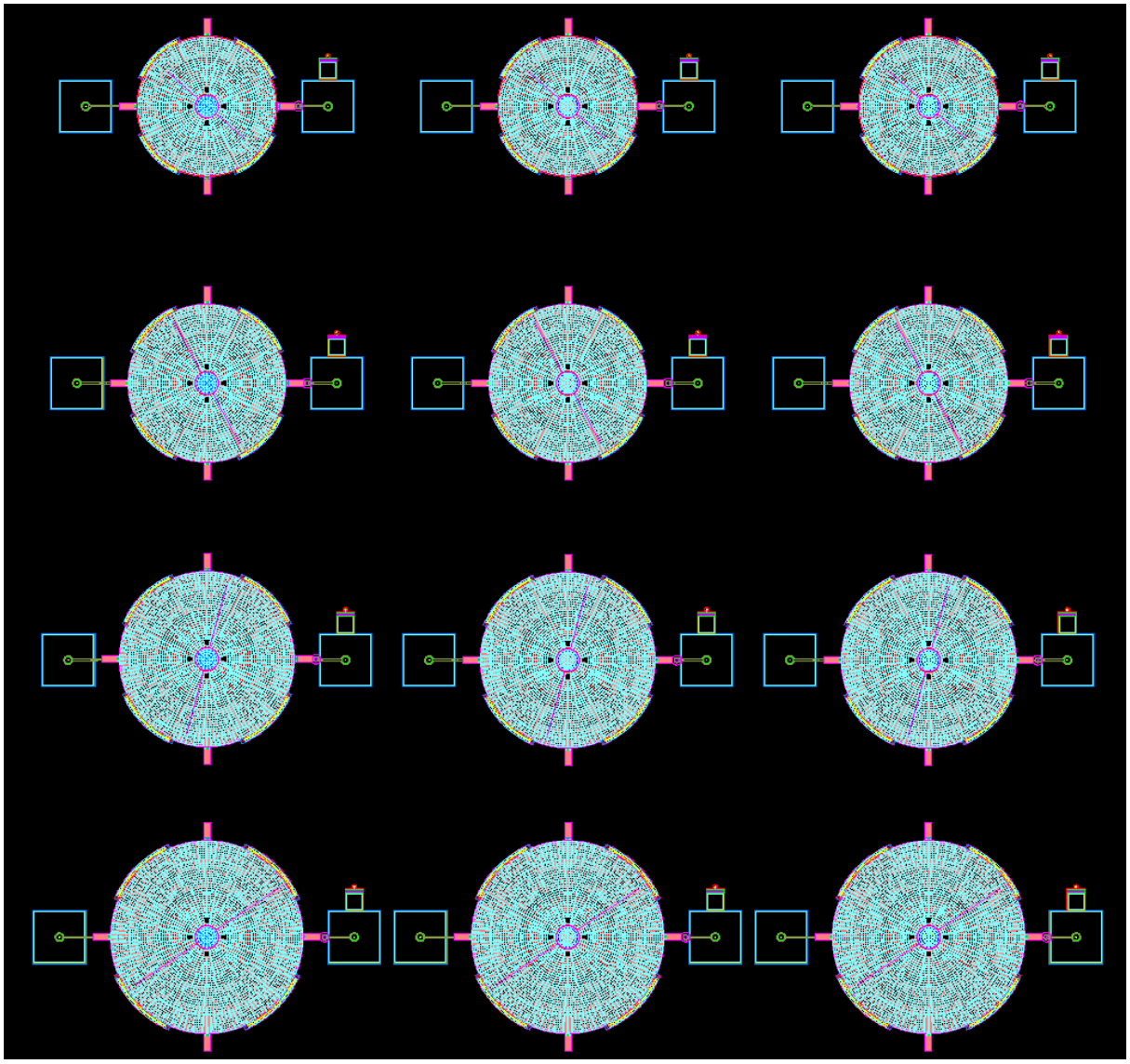

Figure 20, AutoCAD drawing for newly designed valves

Conclusion:

Existing valve geometries were tested to determine the valve's ability to hold off a given pressure with an applied voltage. Existing designs were determined to be more 1.83 times more efficient than previous designs, a significant improvement in valve performance. This was attributable to both the larger radius design and the contribution of trapped oxide in the valve center. Additionally, newer valve designs were proposed, which should be 2.82 times more efficient than current valve geometries, and 5.17 times more efficient than older valve designs. This improved efficiency should lower the power requirement for the device, enabling a smaller battery to be used, decreasing the size of the overall MGA package. Future work includes fabricating the new valve designs and testing their performance, along with analyzing their overall integration with the MGA package.

References:

1 P Galambos, J Lantz, M Baker, M McClain, G Bogart, RJ Simonson, Active MEMS Valves for Flow Control in a High Pressure Micro-Gas-Analyzer, JMEMS, available online soon

2 P Lewis, R Manginell, D Adkins, R Kottenstette, D Wheeler, S Sokolowski, D Trudell, J Bynres, M Okandan, J Bauer, R Manley, G Fry Mason, Recent advancements in gas-phase Microchemlab, IEEE Sensor Journal, 2006

3 C Lu, W Steinecker, W Tian, M Obony, J Nichols, M Agah, J Potkay, H Chan, J Driscoll, R Sacks, K Wise, S Pang, E Zellers, First generation hybrid MEMS gas chromatograph, Lab Chip, 2005

Figure 1 and Figure 6 from Galambos et al. Active MEMS Valves for Flow Control in a High Pressure Micro-Gas-Analyzer

Figure 4 from Standard Summit Design Manual

DISTRIBUTION

1 David Bonner – 842 Meander Drive, Walnut Creek, CA 94598 dgbonner@ucdavis.edu (electronic copy)

1	MS0892	Matthew Moorman	1716 (electronic copy)
1	MS0892	Robert Simonson	1719 (electronic copy)
1	MS0899	RIM-Reports Management	9532 (electronic copy)
1	MS1069	Michael Baker	1719 (electronic copy)
1	MS1080	Keith Ortiz	1719 (electronic copy)
1	MS1080	Paul Galambos	1719 (electronic copy)
1	MS1425	Alan Staton	1716 (electronic copy)


Sandia National Laboratories